



Synthesis of nickel nanoparticle using ionic liquid based extract from *Polygonum minus* and their applications

Habib Ullah^{a,b,*}, Cecilia Devi Wilfred^{a,b,*}, Maizatul S. Shaharun^b

^aFundamental and Applied Science Department, Universiti Teknologi PETRONAS, Bandar Seri Iskandar, 31650, Tronoh, Perak Malaysia, email: habibullah_kust@yahoo.com (H. Ullah), cecili@utp.edu.my (C.D. Wilfred)

^bCenter of Research in Ionic Liquids, Universiti Teknologi PETRONAS, Bandar Seri Iskandar, 31650, Tronoh, Perak Malaysia, email: maizats@utp.edu.my (M.S. Shaharun)

Received 2 November 2017; Accepted 12 August 2018

ABSTRACT

In the present work, 1-ethyl-3-methyl imidazolium chloride [C_3MIM]Cl combine with ultra-sonication was applied for extraction of bioactive compounds from *Polygonum minus*. The extract was used to synthesize nickel nanoparticles (Ni NPs). Synthesis was confirmed by UV/Vis spectrophotometry. The Ni NPs were characterized by X-ray diffraction (XRD), Fourier Transformed Infrared (FTIR) spectroscopy and thermogravimetric analysis (TGA). The morphology was identified by Field Emission Scanning Electron Microscopy (FESEM) and the particle size and zeta potential were analyzed by dynamic light scattering (DLS). Nickel nanoparticles were used for degradation of methyl red, methyl orange, methylene blue and degraded 98% of all dyes in time interval of 5, 5 and 10 min respectively. The synthesized nickel nanoparticles were found to be highly effective against three different bacteria such as *Aeromonas hydrophila* (AH), *Escherichia coli* (EC), *Staphylococcus aureus* (SA) in disc diffusion methods at various concentrations.

Keywords: Ultrasonic cavitation; Ionic liquids; Nickel nanoparticle; photo degradation; Anti-bacteria activities

1. Introduction

Nanoparticles become an active area of research and play a significant role in the various fields such as drugs delivery and renovating medicine etc. [1]. Nickel nanoparticles found varieties of significant application in the field of magnetic fluids, plastics coating, identification of anti-cancer mechanism [2] and catalysis [3]. Previously, nickel nanoparticles have been synthesized by various chemical techniques such as electrochemical techniques [4], metal salt reduction [5], metal evaporation-condensation [6] and irradiation [7]; these methods are intensive in energy, time-consuming, and show toxicity. In order to overcome these limitations, an alternative technique involving reduction of the metal particles to the nanoparticle from biological methods [8]. M.Irfan. et al. synthesized gold nanoparticles using 1-Eth-

yl-3-methylimidazolium chloride as extract-ant from *Elaseis Guineensis*. The nanoparticles were confirmed by UV spectroscopy. TEM image showed the average particles size of 20 nm. The author also used 1-Ethyl-3-methylimidazolium bromide for extraction of flavonoids from *Elaseis Guineensis* for synthesis of gold nano particle and obtained average size of 13.30 nm [9]. In biological methods various resources were used such as, micro-organism and plant extract. There is no reported application of ionic liquid (IL) extract for the synthesis of nickel nanoparticles. We were interested in the potential of ionic liquids, as a solvent to extract phenolic compounds from lignocellulosic biomass and took advantage of ionic liquid as the best solvent. Ionic liquids are best solvent for extraction, which reduces solvent waste, minimizing exposure to hazardous vapors and environmentally friendly. For these advantages their best properties ionic liquids thermally stability, negligible vapor pressure, high heat absorbance capacity and low flammability [10].

*Corresponding author.

Ultrasonic cavitation provides three beneficial aspects such as cavitation bubble, mechanical function and thermal effect, which is maximally utilized in the extraction process and results into the relatively high extraction efficiency. *Polygonum minus* is an aromatic plant with a pleasant smell and is used as cosmetic, anti-oxidant, anti-bacterial activity, flavoring and perfume industry [11]. Traditionally, it was used as herbal medicine which cures the digestive disorder, body aches and dandruff [12]. *P. minus* contains a large amount of essential oil. Essential oils have gained special attention among secondary metabolites because it is used in pharmaceutical, sanitary, cosmetics, food and other agro-based industries as fragrance agents. In addition, they have exploited aromatherapy and in photo therapy.

Dyes are considered as toxic being not degraded by conventional degradation process [13]. Some of these e.g. methyl orange, methyl red, and methylene blue are widely used in industries such as textile, printing, paper and cosmetic [14]. Amongst others, nanoparticles have been used in the degradation of dyes [15]. The Ni NPs showed effective biological activity against bacteria [16]. Anti-bacterial activity depends on the nature of bacterial strain. Bacteria are classified into two type gram positive and gram negative. The gram-positive bacteria have thick cell wall while the gram- bacteria have a thin cell wall.

The main objective of the present work to synthesize a novel, fast and eco-friendly synthetic method for nickel nanoparticles using ionic liquids based ultrasonic-assisted (ILUAE) extraction from *Polygonum minus*. The activity of as-synthesized Ni NPs was tested, against bacteria and photo degradation of dyes.

2. Experimental

2.1. Material

Nickel nitrate $\text{Ni}(\text{NO}_3)_2$ and 1-ethyl-3-methyl imidazolium chloride [C_2MIM] Cl were procured from Merck Millipore, Malaysia. The plant material i.e. *Polygonum minus* was purchased from local market in Malaysia. The microbial organisms were purchased from International Medical University Kuala Lumpur Malaysia. Distilled water was used throughout the experiment.

2.2. Synthesis of nickel nanoparticle

The plant material (*Polygonum minus*) was washed two times with distilled water to remove the impurities, oven dried at 50°C and then ground into powder. To prepare the extract, 5 g powder was mixed with aqueous solution of ionic liquids in the ultrasonic mantle flask at 60°C, 40 W for 20 min. It was then filtered and the clear extract was obtained which is mixture of various compounds such as, flavonoids, terpenoids alkene, alkane and alkaloids as shown in Fig. 1A. These compounds reduce Nickel ion to nickel nanoparticles. To synthesize nickel nanoparticles, 5 mL of the extract was mixed with 0.01 mM aqueous solution of $\text{Ni}(\text{NO}_3)_2$ at 60°C, 50 W for 30 min. The scheme for synthesis of Ni NPs are shown in Fig. 1B. After the reaction, the solution was centrifuged for 5 min at 4000 rpm and washed three times to remove the impurities. The obtained

nanoparticles were vacuum dried at 60°C for one hour and were further characterized.

2.3. Characterization

The Shimadzu UV-2401 double beam instrument was used for UV spectra of Ni NPs at the range between 200–800 nm.

Attenuated total reflection (ATR) spectra were recorded using (FTIR Nicolet 5700, USA). The nanomaterial was placed on diamond crystal and pressed by swivel.

The crystal structure of Ni NPs was determine using X-rays diffractometer (2 θ , 10°–80°, at room temperature) (XPRT-PRO) with Ni-filtered Cu K α radiation. This operated at 0.47° divergent and receiving slits at 40 kV. The crystal size was determined using Scherrer formula.

Mettler Toledo SDTA 10000, TG were used for thermogravimetric analysis of Ni NPs at temperature range 50–900°C at heating rate 10°C/min.

For the determination surface morphology of Ni NPs Zeiss Supra 55VP at 5 kV FESEM instrument were used at various magnification. The nanoparticles were coated with gold water to sufficient for conductivity before image observation. the same sample were analyzed with EDX detector.

The particle size and zeta potential were determined by dynamic light scattering (Malvern DKS). The sample for measurement was dispersed in water and pour in two neck cuvettes.

2.4. Degradation of dyes

The photo degradation of dyes (methyl red, methyl orange and methylene blue) was evaluated by as-synthesized Ni NPs in aqueous medium under UV light irradiation. The dyes solution (One-gram dyes was added into 100 ml deionized water) was introduced in photo reactor and irradiated with light source (lamp type Hamamatsu LC8; lamp power of 0.1W) wavelength λ 500 nm at room temperature. In this experiment, 0.5 mg Ni NPs was added to 10 mL of dyes solutions with initial concentration of 5×10^{-6} M. The mixture was stirred for 20 min in dark to make equilibrium. The distance between light and mixture was about 6 cm. The degradation of dyes was examined using UV/Vis spectrometer. The degradation was calculated by the following equation.

$$\text{Degradation rate (\%)} = \frac{C_o - C}{C} \times 100 \quad (1)$$

where C_o is the concentration of dyes and C of non-degraded dyes.

2.5. Anti-bacterial activity of Ni NPs

Agar diffusion method was used to determine the anti-bacterial activity of Ni-NP using three bacteria i.e. *Escherichia-coli*, *Staphylococcus aureus* and *Aeromonas hydrophilia* [17]. Agar plates were prepared by adding agar media. The plate was cultivated by organisms and three papers were placed in the plate. An amount of 10, 20, 30% sample was added to the respective paper. The plate was incubated for 24 h at 37°C and inhibition zone was measured.

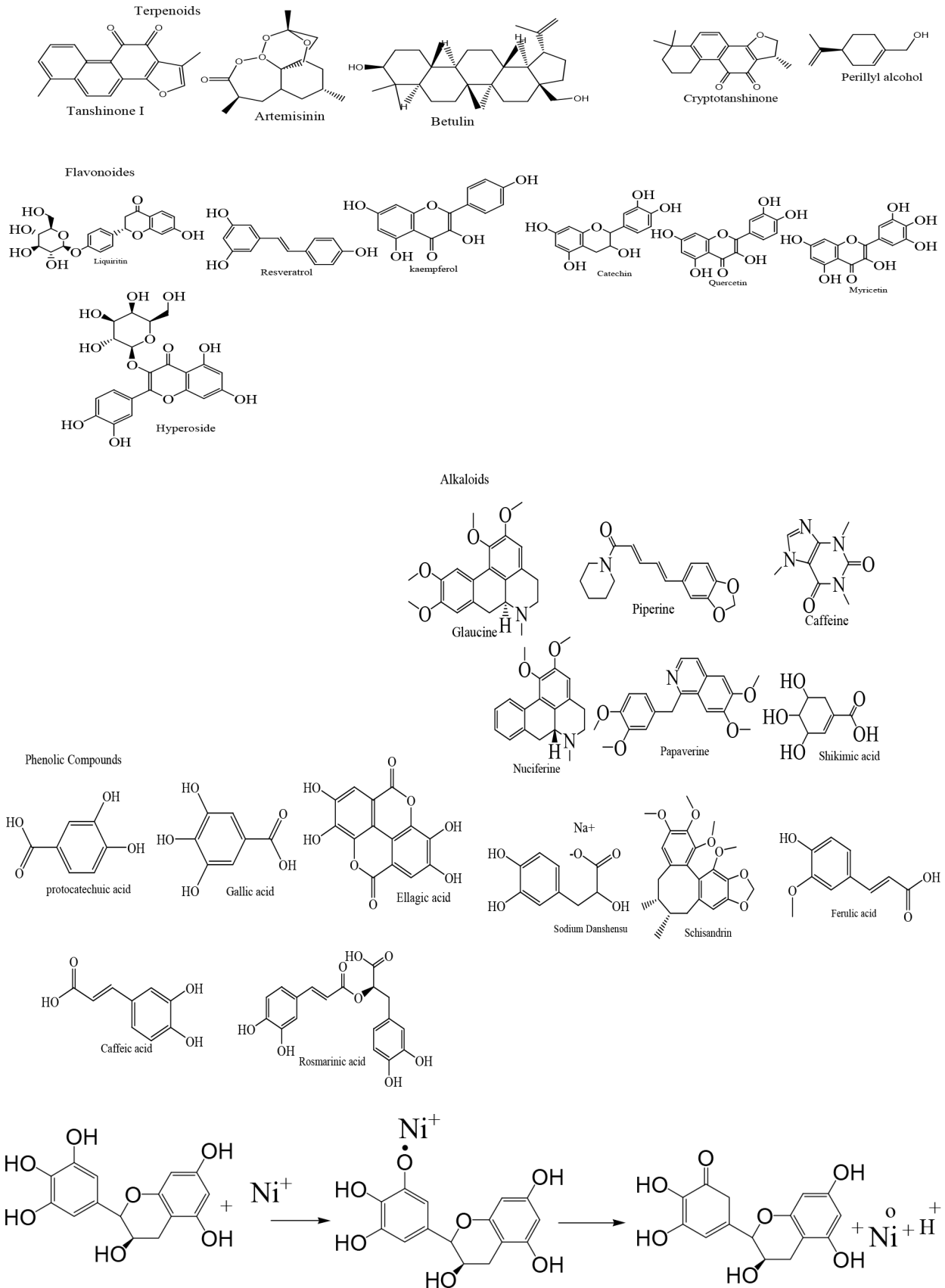


Fig. 1. Structure of bioactive compounds extracted from polygonum minus (A), mechanism for synthesis of Ni NPs (B).

3. Result and discussions

3.1. UV-Vis analysis of Ni NPs

The Formation of Ni NPs from ionic liquids assisted extract based ultrasonic cavitation was confirmed from the color changes; the color of the solution was transformed to light green from deep green. The changes can be detected by UV/Vis diffused reflectance spectrophotometry (DRS) as the synthesized Ni NPs produce a peak at 274 nm as shown in Fig. 2 [8].

Moreover, the increase in the width of the peak at 274 nm evidences the formation of small sized nanoparticles. Similar to our results, the absorption peak at 270 nm indicated the presence of Ni NPs [18]. The wavelength and width of the peak are dependent on the size and shape of the nanoparticles. In Fig. 2, the broad absorption peak is an evidence of the formation of small sized Ni NPs [19].

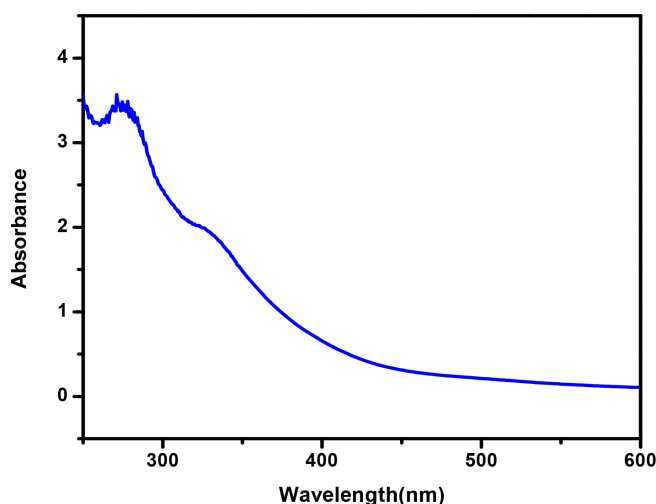


Fig. 2. UV/Visible spectrum of Ni NPs.

3.2. FTIR analysis

The FTIR spectra of plant extract are shown in Fig. 3A. Fig. 3A shows the broad band at 3417 cm^{-1} indicating stretching vibration of OH and the band at 1634 cm^{-1} was assigned to the bending vibration of C=C bonds. The bands at 2931 cm^{-1} and 1378 cm^{-1} are assigned to the C-H stretching and bending vibration of alkyl groups, respectively. The band at 1080 cm^{-1} refers to C-N stretching vibration of aliphatic amines. The band located at 611 cm^{-1} refers to the C-C stretching vibrations of the aromatic ring [20–23]. These bands represent that phenolic, aldehyde, amines, alkene and alkane compounds are present in the plant extract. Fig. 3B shows the FTIR spectra of Ni NPs in which the peak at 2400 cm^{-1} were disappear. These all peaks represent that secondary metabolites of the plant could be responsible for the reduction of nickel ion to Ni NPs [23].

3.3. X-rays diffraction analysis (XRD)

XRD analysis was used to determine the crystalline structure of the synthesized Ni NPs. Fig. 4 shows the XRD pattern

of Ni NPs. Sharp diffraction intensities at 2θ values of 33.3°, 45.5° and 55.5° corresponding to (100), (111) and (200) crystal planes respectively. The pattern suggested face centered cubical structure [24]. The diffraction pattern was in accordance with JCPDS file (card No. 04-0835). The crystallite size based on the Debye-Scherrer equation was 15–23 nm.

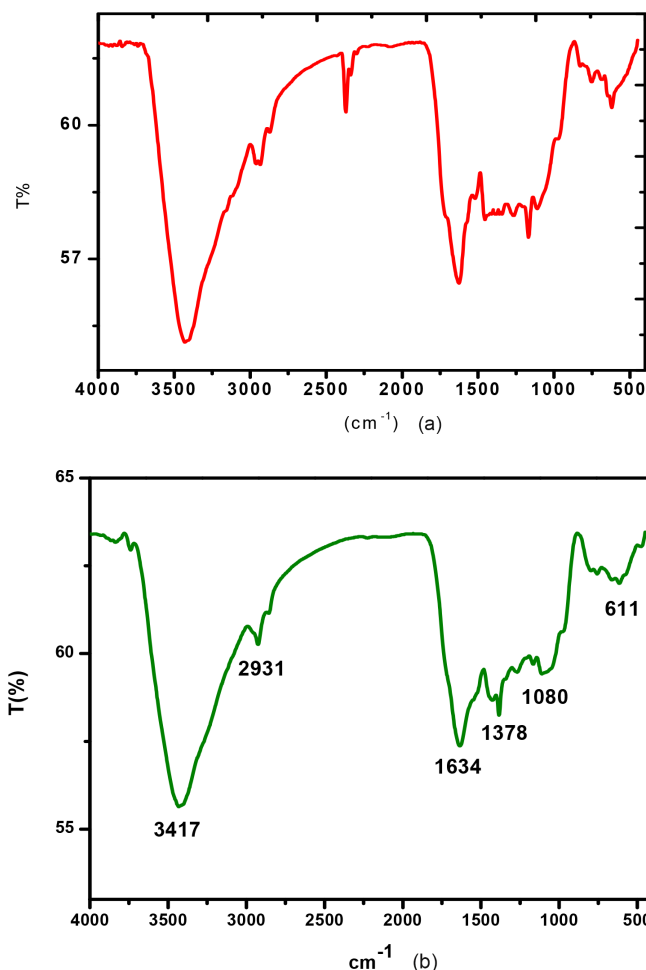


Fig. 3. FTIR spectra of plant extract (A) and Ni NPs (B).

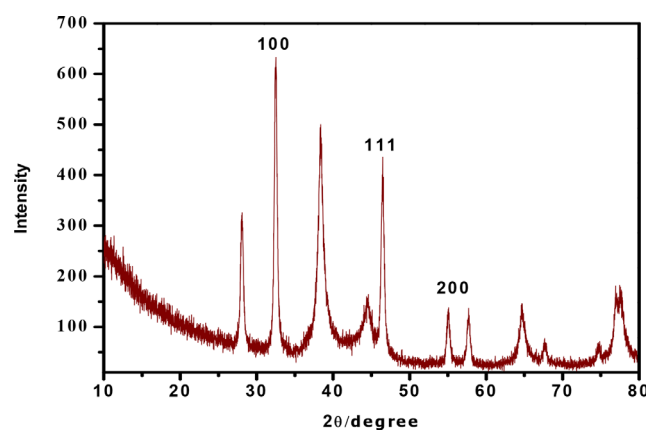


Fig. 4. XRD pattern of Ni NPs.

3.4. Thermogravimetric analysis (TGA)

Fig. 5 shows the TGA result of Ni NPs in the range of 50 to 800°C. The initial weight loss was observed in the temperature range of 100 to 500°C. The TGA curve showed 5% mass loss in the range of 130°C which corresponds to a loss of moisture and less stable molecules. The significant weight loss 80% from 200 to 600°C ascribed the decomposition of bioactive compounds present in *polygonum minus*

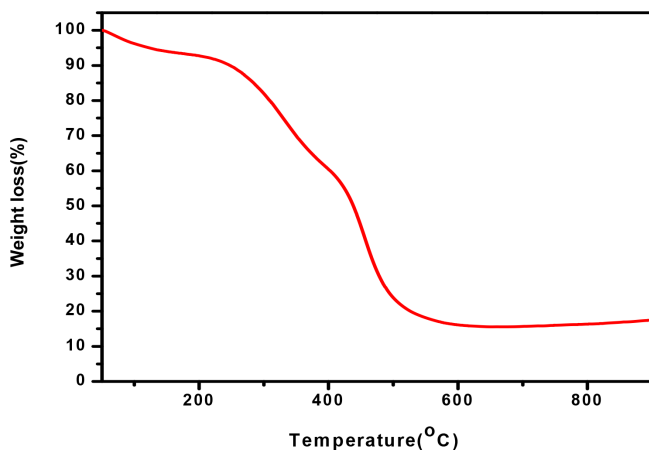


Fig. 5. Thermogravimetric analysis of Ni NPs.

extract. These bioactive compounds act as reducing and capping agents for synthesis of Ni NPs.

3.5. Field emission scanning electron microscopy (FESEM)

The FESEM image is helpful to determine the morphology of the nanoparticles. The Fig. 6A shows that the Ni NPs are spherical in shape in the ranging of 30–100 nm. The morphology was closely supported by the existing literature [25]. The spherical morphology and deagglomeration could be linked with the effect of sonication. The elemental composition of Ni NPs was determined by energy dispersive X-ray analysis (EDX) detector as shown in Fig. 6B reveals the signals in Ni region, confirming the successful synthesis of Ni NPs. The compositional analysis obtained could accurately quantify the Ni contents. Signal of oxygen and carbon result capping the Ni NPs capped bioactive compounds of plant extract. The quantitative analysis was Ni, 43%, O, 20% and C 20.6% respectively, suggesting that bioactive compounds such as phenols, amines and alkane capped the Ni NPs.

3.6. Zeta size and zeta potential

The average size and zeta potential of Ni NPs are shown in Figs. 7a and 7b. The particle size peak showed that the synthesized Ni NPs are polydispersed with an average size diameter of 23.5 nm. Zeta potential is important to determine the surface charge of nanoparticles and long-term stability. The average zeta potential of Ni NPs is -41 mV. This value indicates high stability of the nanoparticles [8]. Hence, these nanoparticles promise a wide range of application in various industries.

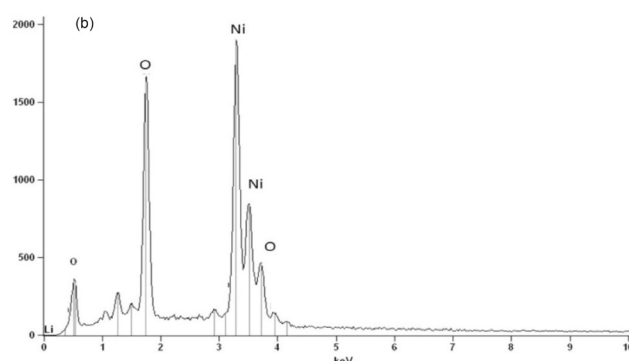
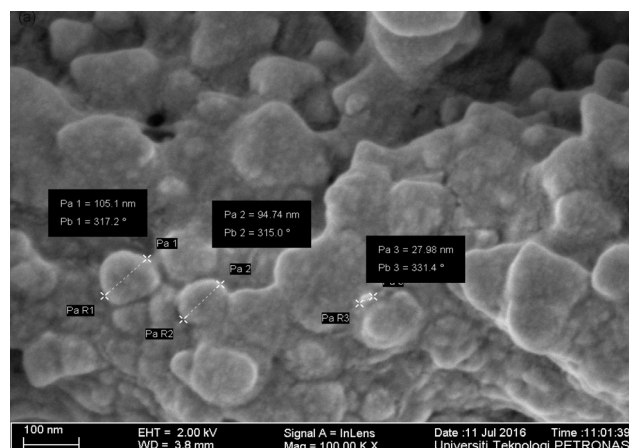


Fig. 6. Field emission scanning electron microscopy of Ni NPs.

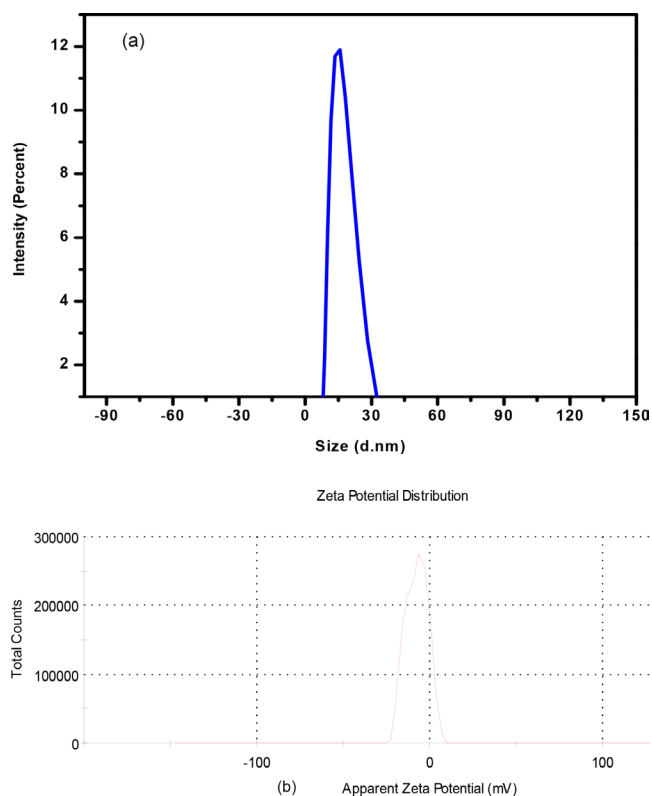


Fig. 7. Particle size A, zeta potential of Ni NPs B.

3.7. Photo degradation efficiency

To establish the photo degradation efficiency of Ni NPs, three different dyes were treated with Ni NPs under UV light. Figs. 8a, b, c show the UV-Vis spectra of photo degradation of MO, MR, and MB dyes before and after treatment with Ni NPs [26–28]. The color of the dyes was disappeared during photo degradation is because of the interactions of the chromophoric groups (double bond=N=N-), present in the dyes, with UV-light. [29]. The spectra showed that the dyes degradation occurred upon addition of the nanoparticles and exposing the solution to UV light (500 tungsten). The sample was taken in time interval of every 2 min centrifuged to settle the NPs and checked by UV/Vis spectroscopy. The dyes MO and MR degraded at five minutes and MB at time interval of 10 minutes as shown in Table 1. The absorption peaks appeared at 466, 460, 664, 590 nm for MO, MR, and MB respectively.

The concentration of dyes was decreased with the increase in reaction time. This shows the successful degradation of 98% of dye, which is better than reported in the literature [30]. The nanoparticles are recycling after centrifugation and reused 5 times and degraded 98%. It is inferred that Ni NPs, synthesized in this study, are good photo catalyst and can be used for the treatment of dyes containing water.

The mechanisms for degradation of dyes can be explained as, smaller the particle size of the nanoparticles and have large surface area and more active site. The Ni NPs has high diffusion without any combination. The photocatalytic activity of nanomaterial depends on the crystal structure, morphology and size of the particles. According to this study when UV-light hit the outer shell electrons of Ni NPs, they absorb energy from light and released from the outermost shell. These electrons produce $\cdot\text{OH}$ radical which is responsible for degradation of dyes as shown in Fig. 8D [31].

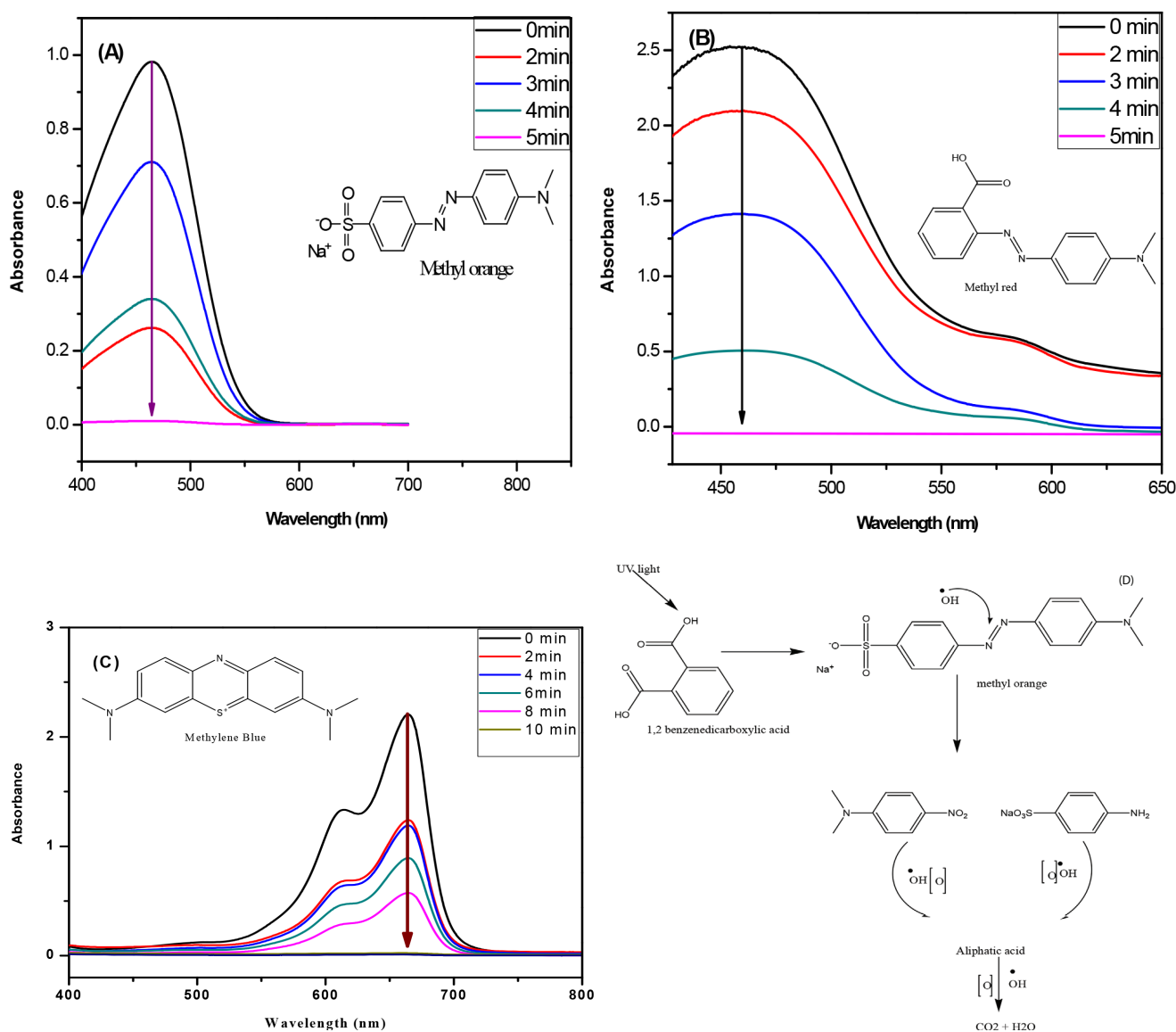


Fig. 8. Time-dependent UV/Vis spectra of different dyes. (A) methyl orange, (B) methyl red, (C) methylene blue, (D) bromophenol blue, mechanism for photodegradation of dyes (D).

3.8. Antibacterial activity of Ni NPs

The Ni NPs synthesized using ionic liquid assisted extract from *Polygonum minus* were tested against three different gram positive and gram negative bacterial strains. The zone of inhibition of 10, 20, and 30% for *Aeromonas hydrophilia*, *Escherichia coli*, and *Staphylococcus aureus* are shown in Table 2 and Fig. 9. The Ni NPs are more efficient against *Escherichia coli* than the *Aeromonas hydrophilia*, *Staphylococcus aureus*. From the Table 1, it is concluded that the nanoparticles have antibacterial properties.



Fig. 9. Anti-bacterial activity of Ni NPs.

4. Conclusions

Nickel nanoparticles have been successfully synthesized by the ionic liquids assisted ultrasonic cavitation extract of *Polygonum minus*. *Polygonum minus* extract can be extracted using IL as solvent under ultrasonic treatment. 23 nm sized Ni NPs are obtained using this mixed technique. The Nano particles were nano crystalline, well dispersed and deagglomerated as confirmed by XRD, FESEM, and DLS. The photo degradation study suggests that Ni NPs are efficient in the removal of methyl orange, methyl red, and methylene blue from aqueous solution in 5–10 min under UV irradiation. Ni NPs exhibited stronger antibacterial activity against gram positive and gram negative bacteria.

Acknowledgements

The authors would like to acknowledge the support provided by Center of Research in ionic liquids (CORIL), and graduate assistantship provided by Universiti Teknologi PETRONAS, Malaysia.

References

- [1] P. Horcajada, T. Chalati, C. Serre, B. Gillet, C. Sebrie, T. Baati, J.F. Eubank, D. Heurtaux, P. Clayette, C. Kreuz, Porous metal-organic-framework nanoscale carriers as a potential platform for drug delivery and imaging, *Nature Mater.*, 9 (2010) 172–178.
- [2] L. Xu, C. Srinivasakannan, J. Peng, D. Zhang, G. Chen, Synthesis of nickel nanoparticles by aqueous reduction in continuous flow micro reactor, *Chem. Eng. Process.: Process Intensif.*, 93 (2015) 44–49.
- [3] M.P. Zach, R.M. Penner, Nanocrystalline nickel nanoparticles, *Adv. Mater.*, 12 (2000) 878–883.
- [4] Y. Hou, H. Kondoh, T. Ohta, Magnetic properties and fabrication of monodisperse FePd nanoparticles, in: *MRS Proceedings*, Cambridge Univ Press, 2004, pp. M2. 3.1.
- [5] Y. Yao, Y. Chen, M. Tai, D. Wang, H. Lin, Magnetic anisotropy effects in nano-cluster nickel particles, *Mater. Sci. Eng. A.*, 217 (1996) 281–285.
- [6] M.-L. Godino-Salido, Preparación, caracterización y propiedades de materiales de carbón con nanoestructuras metálicas, 2014.
- [7] S.M. Helen, M.H.E. Rani, Characterization and antimicrobial study of nickel nanoparticles synthesized from *Dioscorea* (Elephant Yam) by green route, *Int. J. Sci. Res.*, 4 (2015) 216–219.
- [8] S. Sudhasree, A.S. Banu, P. Brindha, G.A. Kurian, Synthesis of nickel nanoparticles by chemical and green route and their comparison in respect to biological effect and toxicity, *Toxicol. Environ. Chem.*, 96 (2014) 743–754.
- [9] M. Irfan, M. Moniruzzaman, T. Ahmad, P.C. Mandal, S. Bhat-tacharjee, B. Abdullah, Ionic liquid based extraction of flavonoids from *Elaeis guineensis* leaves and their applications for gold nanoparticles synthesis, *J. Molec. Liq.*, 241 (2017) 270–278.
- [10] T. Khezeli, A. Daneshfar, R. Sahraei, A green ultrasonic-assisted liquid–liquid micro extraction based on deep eutectic solvent for the HPLC-UV determination of ferulic, caffeic and cinnamic acid from olive, almond, sesame and cinnamon oil, *Talanta*, 150 (2016) 577–585.
- [11] W. Hassan, *Healing Herbs of Malaysia*. Kuala Lumpur: Federal Land Development Agency, in, ISBN 978-983-99544-2-5, 2006.
- [12] P.V.K.K. chiruvella Ilfah, H.A.R.M. Arifullah, A recent review on phytochemical constituents and medicinal properties of kesum (*Polygonum minus* Huds.), *Asian Pacific J. Trop. Biomed.*, 6 (2014) 003.
- [13] N. Yuan, G. Zhang, S. Guo, Z. Wan, Enhanced ultrasound-assisted degradation of methyl orange and metronidazole by rectorite-supported nano scale zero-valent iron, *Ultrason. Sonochem.*, 28 (2016) 62–68.
- [14] J. Fan, Y. Guo, J. Wang, M. Fan, Rapid decolorization of azo dye methyl orange in aqueous solution by nanoscale zerovalent iron particles, *J. Hazard. Mater.*, 166 (2009) 904–910.
- [15] G.M. Whitesides, Nanoscience, nanotechnology, and chemistry, *Small*, 1 (2005) 172–179.
- [16] Y. Xia, Nano materials at work in biomedical research, *Nature Mater.*, 7 (2008) 758–760.
- [17] K. Harish, R. Renu, S.R. Kumar, Synthesis of nickel hydroxide nanoparticles by reverse micelle method and its antimicrobial activity, *Res. J. Chem. Sci.*, 2231 (2011) 606X.
- [18] G. Angajala, R. Ramya, R. Subashini, In-vitro anti-inflammatory and mosquito larvicidal efficacy of nickel nanoparticles phytofabricated from aqueous leaf extracts of *Aegle marmelos* Correa, *Acta tropica*, 135 (2014) 19–26.
- [19] D.D. Evanoff, G. Chumanov, Synthesis and optical properties of silver nanoparticles and arrays, *Chem. Phys. Chem.*, 6 (2005) 1221–1231.
- [20] F. Luo, D. Yang, Z. Chen, M. Megharaj, R. Naidu, The mechanism for degrading Orange II based on adsorption and reduction by ion-based nanoparticles synthesized by grape leaf extract, *J. Hazard. Mater.*, 296 (2015) 37–45.
- [21] Z. Zhuang, L. Huang, F. Wang, Z. Chen, Effects of cyclodextrin on the morphology and reactivity of iron-based nanoparticles using *Eucalyptus* leaf extract, *Ind. Crops Prod.*, 69 (2015) 308–313.
- [22] T. Wang, X. Jin, Z. Chen, M. Megharaj, R. Naidu, Green synthesis of Fe nanoparticles using *eucalyptus* leaf extracts for treatment of eutrophic wastewater, *Sci. Total Environ.*, 466 (2014) 210–213.
- [23] Y.-y. Mo, Y.-k. Tang, S.-y. Wang, J.-m. Lin, H.-b. Zhang, D.-y. Luo, Green synthesis of silver nanoparticles using *eucalyptus* leaf extract, *Mater. Lett.*, 144 (2015) 165–167.
- [24] X. Wu, W. Xing, L. Zhang, S. Zhuo, J. Zhou, G. Wang, S. Qiao, Nickel nanoparticles prepared by hydrazine hydrate reduction and their application in super capacitor, *Powder Technol.*, 224 (2012) 162–167.
- [25] S.-H. Wu, D.-H. Chen, Synthesis and characterization of nickel nanoparticles by hydrazine reduction in ethylene glycol, *J. Colloid Interf. Sci.*, 259 (2003) 282–286.

- [26] J. Del Nero, R. De Araujo, A. Gomes, C. De Melo, Theoretical and experimental investigation of the second hyperpolarizabilities of methyl orange, *J. Chem. Phys.*, 122 (2005) 104506.
- [27] A. Ismail, W. Lau, Influence of feed conditions on the rejection of salt and dye in aqueous solution by different characteristics of hollow fiber nanofiltration membranes, *Desal. Water Treat.*, 6 (2009) 281–288.
- [28] M. Abd El-Latif, A.M. Ibrahim, Adsorption, kinetic and equilibrium studies on removal of basic dye from aqueous solutions using hydrolyzed oak sawdust, *Desal. Water Treat.*, 6 (2009) 252–268.
- [29] N.M. Aljamali, Review in azo compounds and its biological activity, *Biochem. Anal. Biochem.*, 4 (2015) 1.
- [30] Y. Sha, I. Mathew, Q. Cui, M. Clay, F. Gao, X.J. Zhang, Z. Gu, Rapid degradation of azo dye methyl orange using hollow cobalt nanoparticles, *Chemosphere*, 144 (2016) 1530–1535.
- [31] Z.U.H. Khan, A. Khan, A. Shah, P. Wan, Y. Chen, G.M. Khan, A.U. Khan, K. Tahir, N. Muhammad, H.U. Khan, Enhanced photo catalytic and electro catalytic applications of green synthesized silver nanoparticles, *J. Molec. Liq.*, 220 (2016) 248–257.